Impact of Wind on Stormwater Pond Particulate Removal

Hrund Ólöf Andradóttir, Ph.D.[1]

Abstract: Stormwater ponds provide cost and space-efficient treatment of urban runoff via gravitational settling. The goal of this paper was to quantify different mechanisms by which wind can affect the particle removal efficiency of a shallow retention pond. An analytical bulk model was developed and validated numerically against total suspended solids (TSS) measurements in a small (0.3 ha), optimally designed oval pond during four runoff events with 7–11 m/s winds. Simulations highlighted wind as an effective mixing mechanism, lowering the removal of medium silt particles by 10–20% from ideal plug flow, and severely constraining the removal of small clay and silt particles (<6 μm). Initial background concentrations of <12 mg/L TSS were positively correlated with wind speed 5 h prior to the event, indicative of localized wind resuspension. A widespread remobilization of bed sediments was found unlikely in a 1.7-m deep, 112-m fetch pond. A stirred reactor with 60% effective volume is proposed as a first order tool to assess the treatment performance of ideally structured ponds in areas with strong, unobstructed winds. **DOI:** [10.1061/(ASCE)EE.1943-7870.0001221.](#) *This work is made available under the terms of the Creative Commons Attribution 4.0 International license, [http://creativecommons.org/licenses/by/4.0/.](#)*

Author keywords: Particle size; Resuspension; Settling; Short-circuiting; Stormwater pond; Treatment efficiency; Wash loads; Wind mixing.

Introduction

Stormwater ponds have been built worldwide to protect sensitive receiving waters from pollutants in runoff. The main removal process in such systems is gravitational settling. Many toxic pollutants, such as heavy metals and polyaromatic hydrocarbons, have a strong affinity for particulate form and are efficiently removed via settling (Pitt et al. 1995; Hossain et al. 2005). Optimal treatment is achieved when the system acts as a slow moving plug flow reactor, where all particles leave the pond in a singular residence time and particle deposition is not hindered by water turbulence. In real systems, however, a combination of preferential pathways, short-circuiting, mixing, and dead zones contributes to the fact that only part of the volume is effective in treatment, thus reducing the treatment performance. Historically, hydraulic inefficiencies have been quantified in relation to structural design parameters, such as length-to-width ratios and inlet and outlet configurations, or alternatively vegetation cover (e.g., Persson 2000; Li et al. 2007). More recently, numerical and field studies have suggested that wind may be an important hydraulic driver, even in very small (0.3 ha) stormwater ponds (Andradóttir and Mortamet 2016; Bentzen et al. 2008). On one hand, wind-induced currents have been quantified as 10 to 100 times faster than those associated with in- and outflows, promoting short-circuiting. On the other hand, wind has been identified as an efficient mixing mechanism, generating vertical mixing within hours, and basin-scale mixing (BSM) within the typical nominal flushing time of 1 day. Effective mixing dilutes pollutant concentrations, which may, in turn, counteract the short-circuiting. The combined effect of wind-induced extreme short-circuiting and basin-scale mixing has resulted in a 30–40% reduction in nominal residence time (Bentzen et al. 2008).

Wind-induced turbulence affects the rate of removal by continuously redistributing particles over water depth. Small clay particles may never settle, forming wash loads (e.g., Li et al. 2007). Wind-induced shear stress may resuspend particles from the bed, known to contribute to a background concentration in large (3,500 ha), shallow (1.5 m) lakes (Bengtsson and Hellström 1992). Wind waves are the dominant resuspension mechanism in shallow regions, whereas wind-induced currents may be more important in deep water (Katchhwal et al. 2012). Wind-driven resuspension and mixing were found to reduce the total suspended solids (TSS) removal by 20–50% in two 0.24-ha, 0.4–0.5-m-deep wet detention ponds based on three-dimensional (3D) hydrodynamic-sediment transport modeling (Bentzen 2010).

The goal of this research was to quantify four mechanisms by which wind can decrease the particle removal efficiency of a shallow stormwater detention pond, as compared to idealized plug flow. The mechanisms were (1) wind stirring (WS), by which the sediments are mixed vertically over the pond; (2) basin-scale mixing (BSM); (3) short-circuiting (SC), resulting in a reduction in the effective volume (EV) of the pond; and (4) resuspension, resulting in an increase in the background concentration (BC) of fine particles. To compliment recent numerical modeling and experimental field studies (Bentzen et al. 2008, 2009; Bentzen 2010; Andradóttir and Mortamet 2016), this paper develops and tests a physically based analytical bulk model to serve as a simple assessment tool for event mean removal performance in wind driven shallow systems. The paper is organized as follows: first, the theory of wind in the context of particulate transport and removal is reviewed. Then, an analytical model is introduced that quantifies removal inefficiencies associated with the separate mechanisms. Last, the numerical counterpart of the model is validated against TSS measurements during four runoff events, spanning a range in hydraulic and seasonal meteorological conditions. By comparing model simulations to measurements, the model applicability and importance of background concentrations are assessed. The Víkurvegur pond in suburban Reykjavík was chosen as the study site. The long-term monitoring of the pond indicated that treatment efficiencies were lower than anticipated. The pond hydraulic regime has been found to be strongly affected by the wind (Andradóttir and Mortamet 2016). This research was initiated by the local utility Orkuveita Reykjavíkur.

[1]Professor, Faculty of Civil and Environmental Engineering, Univ. of Iceland, Hjardarhagi 2-6, IS-107 Reykjavík, Iceland. E-mail: hrund@hi.is

Theoretical Background

The one-dimensional transport equation for the depth-averaged suspended sediment concentration, C, is

$$\frac{\partial C}{\partial t} + U_x \frac{\partial C}{\partial x} = \frac{\partial}{\partial x}\left(D_x \frac{\partial C}{\partial x}\right) - S + E \tag{1}$$

Here, U_x = advective speed along the pond length axis; D_x = longitudinal shear flow dispersion coefficient; S = decay term via gravitational settling; and E = source of sediments eroded from the bed.

Settling and Pe_z

Spherical particles with diameter, d, and specific density, s, are generally assumed to settle according to Stokes law (Andral et al. 1999), with a speed of

$$W_s = \frac{(s-1)gd^2}{18\nu} \tag{2}$$

Here, g = gravitational acceleration and ν = kinematic viscosity of water. The characteristic timescale for settling is the time to travel over the water depth, H, i.e.

$$t_s = \frac{H}{W_s} \tag{3}$$

The settling term, S, in Eq. (1) depends on the vertical Peclet number, which describes the strength of particle deposition relative to vertical mixing, i.e.

$$Pe_z = \frac{W_s H}{D_z} \tag{4}$$

The depth-averaged vertical diffusion coefficient in the water column scales on a representative vertical shear velocity, u_*, as

$$D_z = \frac{1}{15}u_* H \tag{5}$$

In a wind-dominated system, momentum transfer is driven by the surface shear velocity:

$$u_{*s} = \sqrt{\frac{\tau_s}{\rho}} \approx 1.3 \times 10^{-3} W_{10} \tag{6}$$

Here, τ_s = fully developed wind shear stress; W_{10} = measured wind speed at a 10-m elevation over the ground; and ρ = density of water. Eq. (6) represents a theoretical maximum. The wind response in small systems may be lower due to fetch limitations and sheltering. To account for this, the representative shear stress may be taken as the average of surface and bed shear velocity produced by wind-driven currents, or

$$u_* = \frac{u_{*s} + u_{*b}}{2} = k_1 u_{*b} \tag{7}$$

The coefficient k_1 is affected by land slope and vegetation cover around the pond. It can be assessed from velocity measurements in the pond, as discussed later in this paper [Eq. (35)]. Eq. (4) may be rewritten as

$$Pe_z = 15\frac{W_s}{k_1 u_{*b}} \tag{8}$$

If $Pe_z \geq 20$, then particles are unaffected by vertical mixing. The settling term is a constant, resulting in a linear deposition of particles with time (Dhamotharan et al. 1981). Alternatively, if $Pe_z \leq 0.2$, then particles are continuously redistributed over depth and the settling term is represented as a first order decay.

Particle Fall Number

The key parameter governing the removal in a stormwater pond is the particle fall number (Li et al. 2007). Defined as the ratio between the nominal residence time, t_n, and particle settling time, i.e.

$$N_f = \frac{t_n}{t_s} \tag{9}$$

it compares the strength of advective transport [left hand side, Eq. (1)] to settling, S. The nominal residence time represents the average time particles stay in the system and is the ratio between the pond volume, V, and throughflow rate, Q, i.e.

$$t_n = \frac{V}{Q} \tag{10}$$

In transient storage systems, Q may be taken as the average of inflow rate, Q_{in}, and outflow rate, Q_{out}.

Inverse Overflow Rate

The particle fall number may be written as

$$N_f = \frac{W_s}{Q/A} = W_s \frac{t_n}{H} \tag{11}$$

The governing hydraulic parameter determining the removal of particles of different diameters is the residence time to water depth, t_n/H, which will be referred to hereafter as the *inverse overflow rate*, defined as the ratio of surface area and throughflows, A/Q, which is not affected by water depth.

Hydraulic Regime and Pe_x

The parameter governing the hydraulic regime in Eq. (1) is the longitudinal Peclet number, which compares the strength of transport by advection to diffusion $(U_x L/D_x)$. In the context of particulate removal, the advective speed is that of throughflows across width and depth $(U_x = Q/BH)$. Incorporating longitudinal dispersion associated with vertical shear, a conservative estimate of the Peclet number can be taken as (see Andradóttir and Mortamet 2016)

$$Pe_x = \frac{QL}{5.93 u_* BH^2} \tag{12}$$

If $Pe_x < 2$, then dispersion dominates throughflows, and the pond mimics a continuously stirred reactor more than plug flow (Tsai and Chen 2013). The Peclet number can be rewritten in terms of shear bed velocity and inverse overflow rate as

$$Pe_x = \frac{1}{5.93(k_1 u_{*b})}\frac{H}{t_n}\left(\frac{L}{H}\right)^2 \tag{13}$$

Pe_x is therefore sensitive to the pond length-to-depth aspect ratio, L/H.

Erosion

Sediments from the bed may be resuspended into the water column if the wind-induced bed shear stress, τ_b, exceeds the critical shear stress for erosion, τ_{cr}, i.e.

$$\chi = \frac{\tau_b}{\tau_{cr}} = \left(\frac{u_{*b}}{u_{*cr}}\right)^2 > 1 \qquad (14)$$

The critical shear stress can be estimated based on empirical relationships, such as the Fischenich (2001) formula for silt

$$\tau_{cr} = 0.25 d_*^{-0.6} \rho g(s-1) d \tan \phi \qquad (15)$$

A friction angle, $\phi = 35°$, is representative of fine sediments in tailing ponds (Kachhwal et al. 2012). The nondimensional grain size diameter is

$$d_* = d \left[\frac{(s-1)g}{\nu^2}\right]^{13} \qquad (16)$$

The erosion rate of suspended sediments from the bottom may be represented as (Bengtsson and Hellström 1992)

$$E = C_e(\chi - 1)^n \qquad (17)$$

The erosion coefficient, C_e (g/m²/h), and exponent, $n = 1$–2, depend on site characteristics, such as bed sediments, grain size, and consolidation time. A coupled 3D sediment transport-hydrodynamic model accounting for spatial variability in water depth and wind driven waves may be needed to assess erosion accurately in small, fetch-limited systems (e.g., Bentzen et al. 2009; Bentzen 2010).

Analytical Assessment

Model Development

An analytical steady state particulate removal model that accounts sequentially for various wind effects in a stormwater pond was derived from Eq. (1). The three key model input parameters were (1) particle diameter d; (2) inverse overflow rate; t_n/H; and (3) wind shear bed velocity u_{*b}. These parameters, along with a selection of others, allow assessing the nondimensional parameters presented in the theoretical background section (Table 1).

The total removal efficiency was assessed by solving Eq. (1) for the steady state outflow concentration, C_{out}, and assess how much it deviated from that of the inflow, C_{in}, i.e.

$$R.E. = 1 - \frac{C_{out}}{C_{in}} \qquad (18)$$

No Wind (NW)
The Hazen (1904) model represents the most ideal conditions possible in a given system. First, the hydraulic regime is plug flow ($D_x \to 0$), where particles are evenly distributed across the width

Table 1. Analytical Model Input Parameters

Parameter	Description	Derived parameters
d	Particle diameter (μm)	W_s, N_f
$t_n/H = A/Q$	Pond inverse overflow rate (day/m)	N_f, SCI
u_{*b}	Wind shear bed velocity (m/s)	Pe_x, Pe_z, SCI, a
$k_1 = u_*/u_{*b}$	Ratios of depth-average to bed shear velocity	Pe_x, Pe_z
$k_2 = U_x/u_{*b}$	Ratio of wind driven water speed to bed shear velocity	SCI
L/H	Pond length-to-depth aspect ratio	Pe_x, SCI
e	Pond effective volume	a

and leave the system in a singular time, $t_n = L/U_x$. Second, no background concentrations or sediment sources are present in the basin. Third, water turbulence does not affect particle deposition ($Pe_z > 20$). Under such ideal conditions, settling occurs as a zeroth order decay process ($S = C_{in}/t_s$). The solution of Eq. (1) is a linear deposition of particles with time. The maximum theoretically achievable hydraulic removal efficiency is

$$R.E._h = \frac{t_n}{t_s} = N_f \qquad (19)$$

In the ideal no-wind model, all particles, and particle bound pollutants, may be removed if $N_f \geq 1$. Different sources of inefficiencies, generating deviations from this model, are considered sequentially in the next sections.

Wind Stirring
Wind-induced turbulence promotes vertical mixing. If $Pe_z \leq 0.2$, wind may redistribute particles throughout the water column. In this case, the gravitational settling process is better represented as a first order reaction [$S = C/t_s$, Eq. (1)]. The removal efficiency increases exponentially with particle fall number:

$$R.E._h = 1 - \exp(-N_f) \qquad (20)$$

Basin-Scale Mixing
Assuming that wind mixing is strong enough so the pond behaves to a large extent like a stirred reactor, with effective longitudinal and vertical mixing of particles ($Pe_x < 2$, $Pe_z \leq 0.2$), the steady state removal efficiency is

$$R.E._h = \frac{N_f}{N_f + 1} \qquad (21)$$

Effective Volume
A natural system rarely functions as a completely mixed reactor, but rather as a partial mixed reactor with elements of short-circuiting. The bulk effect of short-circuiting and mixing is that part of the pond volume may be ineffective in transport. The effective volume ratio is generally determined from tracer tests as

$$e = \frac{V_{effective}}{V_{total}} = \frac{t_{50}}{t_n} \qquad (22)$$

where t_{50} = timescale when 50% of the mass has exited the system. Eqs. (21) and (19) may be adapted for effective volume by multiplying N_f with e, resulting in

$$R.E._h = \frac{N_f}{N_f + 1/e} \qquad Pe_z \leq 0.2 \qquad (23)$$

$$R.E._h = N_f e \qquad Pe_z \geq 20 \qquad (24)$$

Short-Circuiting
Another way of modeling partial basin mixing is by using the time-scale for particles short-circuiting across the length of a pond, L, with water speed that scales on shear bed velocity, $U_x = k_2 u_{*b}$, i.e.

$$t_{sc} = \frac{L}{k_2 u_{*b}} \qquad (25)$$

The constant k_2 may be assessed from field data [see e.g., Eqs. (34) and (35)]. The nondimensional short-circuiting index may be defined as (Andradóttir and Mortamet 2016)

$$SCI = \frac{t_{sc}}{t_n} \quad (26)$$

Assuming a portion, a, of the mass short-circuits as plug flow with time $t_{sc} < t_n$ after which the remaining portion is well mixed with residence time t_n, the WS and BSM models predict a combined hydraulic removal efficiency of vertically mixed particles ($Pe_z \leq 0.2$) as

$$R.E._h = 1 - \exp(-N_f SCI) \times \frac{aN_f + 1}{N_f + 1} \quad (27)$$

The model benefit is that it predicts removal as a function of wind response (u_{*b}). Its drawback is that it relies on a new parameter, a, whose relationships with wind speed has not been determined. The model should be applied, and interpreted, with care. A closure that ensures that the mean residence time equals to et_n is used

$$a = SCI + 1 - e < 1 \quad (28)$$

Notice that with this closure, the SC model [Eq. (27)] does not asymptote to the EV model [Eq. (23)] with $SCI \to 0$. In this paper, the SC model is used to showcase a possible transition between the NW and EV models with increasing wind forcing. The removal of partially stirred particles ($0.2 < Pe_z \leq 20$) was assessed by taking a weighted average of Eqs. (24) and (27), with the weighting factor scaling linearly on shear bed velocity.

Background Concentration (BC)

The background concentration, C_*, may be represented as the sum of an initial background concentration, C_0, and a wind-induced time dependent erosion (Bengtsson and Hellström 1992)

$$C_* = C_0 + E \frac{A_e}{A} \frac{t_e}{H} \quad (29)$$

The fraction A_e/A represents the ratio of the total bottom area that is eroded, i.e., because of varying depth and/or wind exposure. Assuming an infinite supply of loose sediments near the bed, then the erosion time, t_e, is the duration of wind exceeding the erosion threshold [Eq. (14)]. However, erodible material is often of limited supply, such that the second term in Eq. (29) may be taken as a constant. The total removal efficiency, accounting for a constant background concentration representing the lowest attainable concentration in a pond, is

$$R.E. = \left(1 - \frac{C_*}{C_{in}}\right) R.E._h \quad (30)$$

This definition highlights the fact that removal efficiency, defined as the proportional reduction in pollution levels from the inflow to the outflow [Eq. (18)], is bounded by the entering pollution. If inflowing concentrations asymptote toward the background concentrations, i.e., $C_{in} \to C_*$, the pond performs no treatment. In the worst case scenario, the pond may act as a source of pollutant if $C_{in} < C_*$. The total removal efficiency may be criticized as an unfair indicator of treatment performance as it does not distinguish between a polluted and clean inflow. It can be argued that the hydraulic removal efficiency, which neglects the background concentration, is a better measure of the achievable removal in the system. The following section focuses on the hydraulic removal efficiency. Background concentrations will be considered in the numerical calibration of field data.

Analytical Model Results

Fig. 1 plots the hydraulic removal efficiency ($C_* \ll C_{in}$) as a function of the particle fall number for four different flow regimes. In the ideal case of no wind [NW, Eq. (19)], all particles are removed within $N_f = 1$. Wind stirring (WS) [Eq. (20)] reduces the particle treatment by 37% for $N_f = 1$. To achieve an 80 and 95% particle removal requires $N_f = 1.6$ and 3, respectively. As N_f is linearly correlated with a pond surface area [Eq. (11)], a 1.6- to 3-times-larger surface area is required to achieve high treatment levels when WS is present, as compared to when it is not. Wind-induced basin-scale mixing [BSM, Eq. (21)] further impairs treatment performance, reducing the removal efficiency by an additional 10–20% from that of the WS model for $N_f = 1$–10. An 80 and 95% removal of particles is attained at $N_f = 4$ and 19. Accounting for the effective volume [EV, Eq. (23)], using $e = 0.6$ from Bentzen et al. (2008) numerical tracer experiments of a wind-dominated stormwater pond reduces the treatment efficiency more moderately, or by an additional 13 and 5% from the BSM model for $N_f = 1$ and 10, respectively. $N_f = 5.6$ and 30 are required to achieve 80 and 95% removal, respectively.

Fig. 2 explores the effect of wind driven shear bed velocity on the hydraulic removal of different particle sizes for a range of hydraulic loading conditions. At low winds ($SCI \geq 1$), removal efficiency is simulated with the NW model [Eq. (19)]. Once wind is strong enough to promote short circuiting ($SCI < 1$), the SC model for exponentially depositing particles [$Pe_z \leq 0.2$, Eq. (27)], or its weighted average with the model for linearly depositing particles [$Pe_z \approx 20$, Eq. (24)], is used. When wind is strong enough to promote longitudinal mixing ($Pe_x < 2$), the EV model [Eq. (23)] applies. For simplicity, e is assumed independent of wind strength [Eq. (28)]. Fig. 2(a) shows that limited wind is required to fully mix clay particles ($d \leq 2~\mu m$) in the vertical ($Pe_z \leq 0.2$ at $u_{*b} \approx 0$). The removal efficiency drops from 10–80% to 6–33% during wind for $t_n/H = 0.5$–4 day/m. Once the shear bed velocity exceeds the critical value of 0.6 cm/s, wind driven currents and waves may resuspend fine materials collected in the shallow sections, further impairing the particulate treatment [not shown, referring to Eqs. (17), (29), and (30). Fig. 2(b) suggests that wind could also severely constrain the removal of fine silt from 90–100% (NW) to 35–81% (EV). A higher shear bed stress is required to remobilize these particles from the bed. Figs. 2(c and d) suggest that a considerable wind may be needed to vertically mix medium ($u_{*b} > 0.2$ cm/s) and coarse silt ($u_{*b} > 0.5$ cm/s). Winds lower the removal efficiency moderately to 72% for medium silt, and 86% for coarse silt according to the EV model for $t_n/H = 0.5$ day/m. To summarize, wind mixing most severely affects the removal of
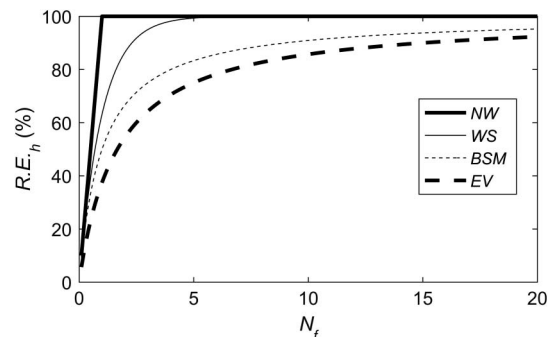

Fig. 1. Analytical hydraulic removal efficiency as a function of particle fall number (NW = no wind; WS = wind stirring; BSM = basin-scale mixing; EV= effective volume)
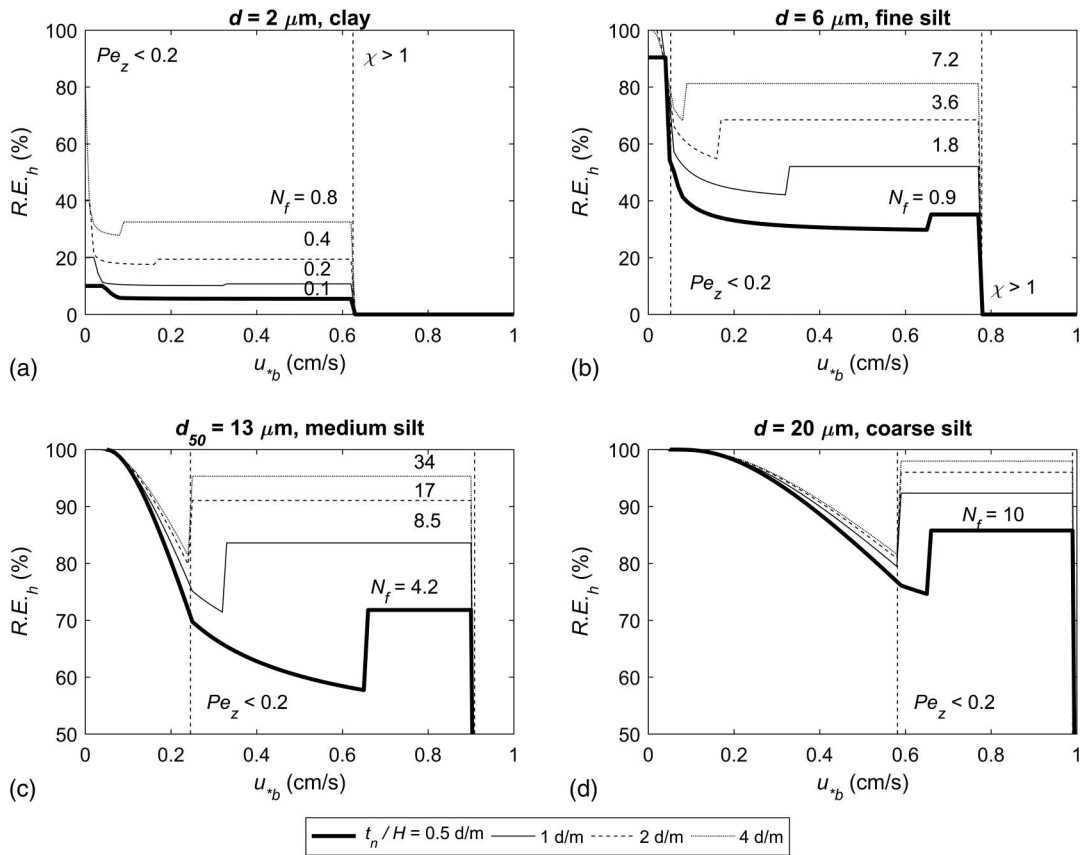
Fig. 2. Hydraulic removal efficiency as a function of shear bed velocity and inverse overflow rate for different particle sizes ($C_* = 0$; $e = 0.6$; k_1, $k_2 = 3$, 5; $L/H = 100$; $s = 2.6$; $\nu = 1.5 \times 10^{-6}$ m^2/s)

small silt and clay particles (<6 μm). Such particles may require weeks to settle. Consequently, fine solids may be only partially removed during a runoff event that lasts hours or one day, contributing to so-called wash loads (or background concentration), both during wet and dry periods. Removal of small particles is important because of their higher toxicity and higher pollutant concentrations (Sansalone and Buchberger 1997). In a structurally well designed pond, wind may constrain up to 30% of the removal of medium silt particles, which are representative of medium grain diameter in runoff. Alternatively, in a pond with high width-to-length ratio or short separation between inlet and outlet, wind mixing may improve the removal efficiency by reducing the pond's inherent structural short-circuiting.

Numerical Counterpart of EV

Eqs. (23) and (30) represent a physically based analytical model that may be used to predict removal efficiencies on an event basis in a small wind-dominated stormwater pond where basin-scale mixing and vertical stirring are effective ($Pe_x < 2$, $Pe_z \leq 0.2$). The key input data are (1) particle size distribution (PSD) of entering runoff; (2) hydraulic flow rates entering the pond ($Q_{in,t}$), and preferably also out of the pond ($Q_{in,t}$); and (3) effective volume, e, and background concentration, C_*, summarizing wind-effects at bulk level. As a first order approximation, e may be taken as 60% based on Bentzen et al. (2008) numerical tracer experiments. The background concentration, however, varies with inflowing TSS and biochemical factors (Kadlec 2000; Barrett 2008), as well as wind [Eqs. (29) and (17)]. Therefore, the model should preferably be tested against field measurements.

The forward difference solution for concentration at the outlet for a given time step, t, associated with particle size classes, j, representing a ratio of total mass, PSD_j, is

$$C_{t+1,j} = \left\{ \frac{Q_{in,t}}{eH_tA_t} PSD_j C_{in,t} - \frac{W_{s,j}}{H_t}(C_{t,j} - PSD_{*,j}C_*) - \frac{Q_{out,t}}{eH_tA_t} C_{t,j} \right\} \Delta t + C_{t,j} \tag{31}$$

The parameters e and C_* are assumed to be time invariant, which is not necessarily the case (see, e.g., Wong et al. 2006). By fitting the numerical solutions to measured TSS in the outflow, the model can be calibrated for e and C_* (and initial concentration C_0) based on the mean diameter d_{50}, for which the PSD of the entering runoff as well as background concentrations is equal to one. Alternatively, particle size classes can be simulated separately and summed up as

$$\sum_j C_{t+1,j} \tag{32}$$

Field Assessment

Site Description

The Víkurvegur wet retention pond treats the surface runoff from the 9-ha mixed residential and light commercial suburb Grafarholt [Reykjavík, Iceland; Fig. 3(a)]. Accounting for an average runoff coefficient of 0.5, the catchment is 4.5 reduced hectares (rha). The oval pond is 112 m long, 26 m wide, and with a design depth of
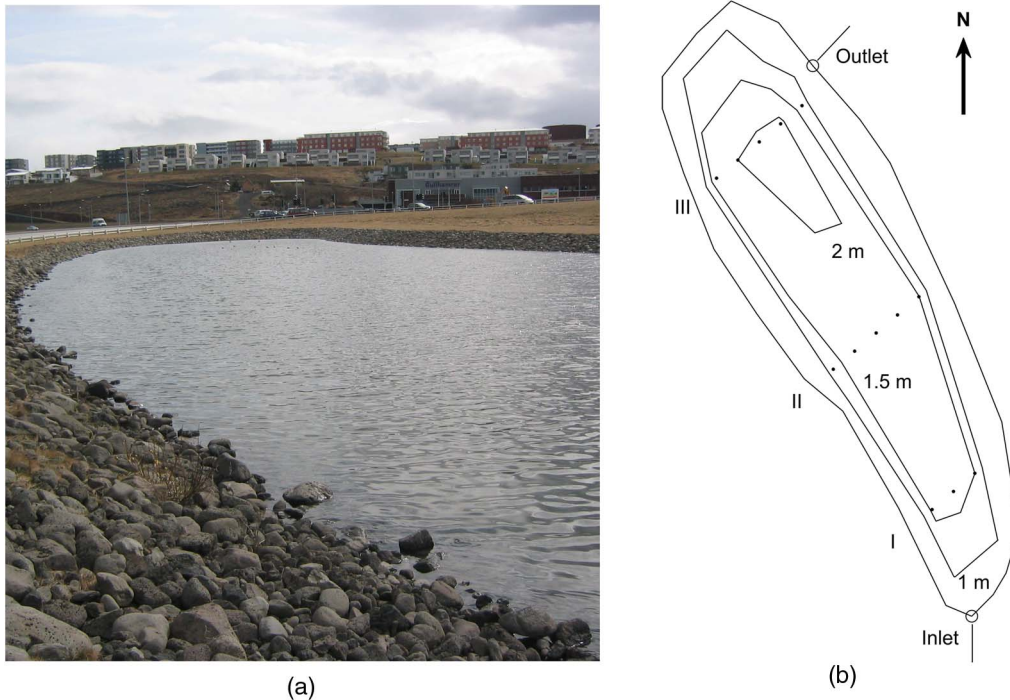
Fig. 3. Víkurvegur pond site: (a) pond with watershed in background (image by Hrund Ólöf Andradóttir); (b) water depth

2 m. A length-to-width ratio, $L/B \approx 4{:}1$, ensures high effective volume (Thackston et al. 1987), i.e.

$$e = 0.84\left[1 - \exp\left(-\frac{0.59\,L}{B}\right)\right] \approx 0.76 \qquad (33)$$

The water inlet situated on the southern end of the pond consists of a submerged 600-mm diameter concrete pipe intruding about 10 m into the pond. The outlet of the pond, situated on the northern end to reduce short-circuiting, consists of a stone trap, 500-mm PEH pipe, and V-shaped overflow structure. The slanted (1:3) side walls are lined with large stones for wave and scour protection. The pond is in a traditional sense overdesigned with a surface area of 650 m² per reduced hectare, a result of a flow diversion made after the pond was built.

The water depth was measured manually with a pole with an accuracy of ±2 cm on April 23, 2009 (reference water level: 52.14 m a.s.l., 0.09 m higher than the design water level), at thirteen stations at 5 m intervals across three transects [dots, Fig. 3(b)]. A thick layer of loose bottom sediments was detected along the transect closest to the inlet. The average water depth there was 1.61 ± 0.11 m, with a maximum depth of 1.72 m, indicative of a 38-cm thick sediment layer. In comparison, the measurement probe hit solid ground at the center of the pond near its outlet, indicative of limited sediment accumulation. The average water depth of the pond was assessed as 1.7 m.

Field Data

Temporal Measurements

Fig. 4 presents the overview of field data collected during four runoff events. The volumetric outflow rate was monitored every 10 min via a spillway, from which the inflow rates were back-calculated based on measured water levels and pond bathymetry (Icelandic Meteorological Office 2009; Gunnarsson and Sigurðsson

2007). The two winter events included both rain and snow, and had higher flowrates than the two rainfall spring events [Fig 4(a)]. During all events, and in particular the lower intensity spring events, outflows persisted for a long time after inflows stopped. The weather station at Úlfarsá recorded at 10-min intervals rainfall, air temperature (T_a), wind speed at 2 m above ground (W_2), and wind direction (θ_w) in an open area approximately 500 m east of the pond inlet (Vista Engineering 2009). Air temperatures were increasing during part of or throughout the events [Fig. 4(b)]. The two winter events and second spring event [Fig. 4(c)] were characterized by strong easterly winds (>10 m/s) followed by more calm southerly winds.

Hourly 1-L water samples were collected in the stormwater sewer by the entrance and outlet of the pond with Liqui-port 2000 autosamplers when runoff rates exceeded 4 L/s, to avoid the data noise associated with the back-calculations of flowrates (Icelandic Meteorological Office 2009). While this threshold reduced the risk of pulling air or stagnant water during dry periods, it restricted the sampling of long tails in the outflow after inflow stopped [Fig. 4(a)]. Selected water samples were analyzed for TSS at the University of Iceland (0.2 μm glass fiber filter), and major elements at the accredited Analytica-AB laboratory (SWEDAC ISO/IEC 17025) located in Luleå, Sweden. Inflowing TSS [heavy boxed lines, Fig. 4(d)] varied from 10 to 100 mg/L between events. Highest TSS concentrations were recorded during the February snowmelt, concurrent with high Na concentrations [Fig. 4(e)]. Concentrations of TSS and Na were moderate during the December rain-on snow event, and low during the two low-intensity spring rain events. The elevated Na concentrations during both winter events indicated the presence of road salt used in cold climates as a deicing agent. The TSS concentrations at the outlet [light circled lines, Fig. 4(d)] varied little within and between events, averaging 9.0 ± 2.7 mg/L (max: 4 mg/L; min: 14 mg/L). Na concentrations in the outflow varied, however, between events. More information on the events selection, water sampling, and chemical analyses of inflowing runoff is presented in Andradóttir and Vollertsen (2015).
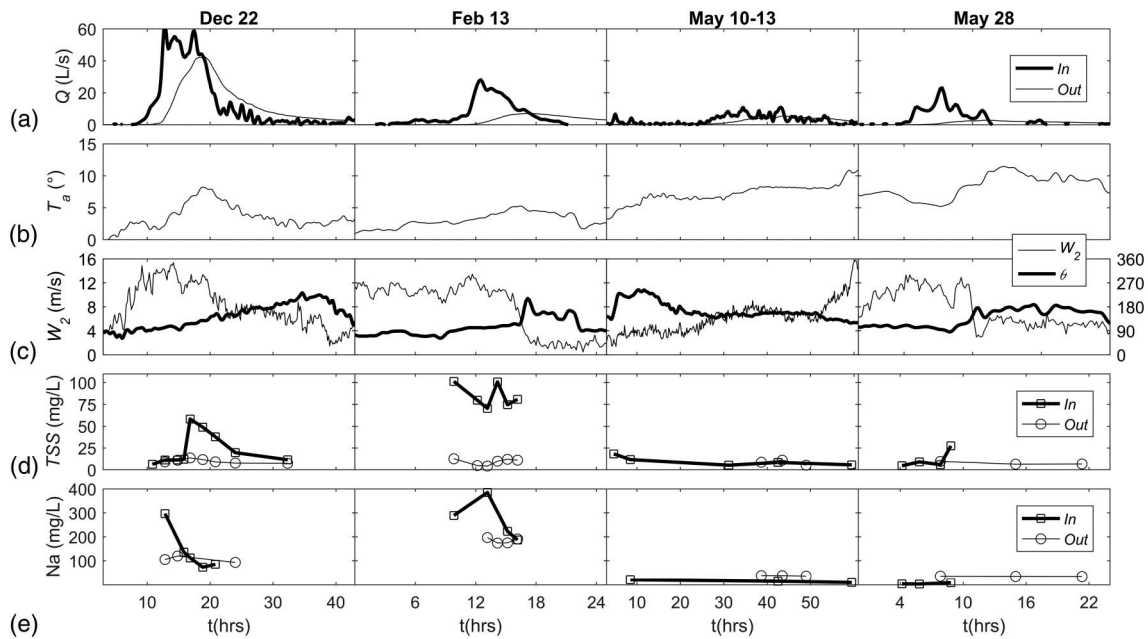
Fig. 4. Event based data: (a) flow rates; (b) air temperature; (c) wind speed and direction; (d) TSS (e) Na concentrations

Wind Metrics

Using the linear regression relationships derived at this site during moderate winds (<8 m/s) and dry weather (Andradóttir and Mortamet 2016), a time series of wind-induced surface (and bed) water speeds along the longitudinal axis of the pond, $U_x(t)$, and associated shear bed velocity, $u_{*b}(t)$, in the center of the pond were projected from measured wind speeds (and directions) as

$$U_x(t) = 0.002W_2(t) \tag{34}$$

$$u_{*b}(t) = k_3 W_2(t) \tag{35}$$

The constant $k_3 = 2.8$, 5.5, and 8.4×10^{-4} for the wind from the east, north-south, and west corresponds to $k_2 = U_x/u_{*b}$ and k_1 in the range of 3–7 and 2–4, respectively. Time series of non-dimensional wind hydraulics metrics were calculated by incorporating these projected water speeds into Eqs. (8), (13), (14), (25), and (26). For this particular pond, wind waves were excluded on the basis that the significant wave height was 1 ± 1 cm (max 8 cm), its wavelength 19 ± 12 cm (max 76 cm) and period 0.3 ± 0.1 s (max 0.7 s) in the center of the pond during the 12 months starting June 1, 2008, according to the Sverdrup-Munk-Bretschneider (SMB) approach. The corresponding wind/wave induced orbital velocities, following Kachhwal et al. (2012), were generally insignificant at 1.7 m below the water surface. While wave shear stress was likely insignificant in the center of the pond, it may have been important locally downwind.

Particle Size and Resuspension

Two 10-liter grab samples were manually collected at the inlet on July 1, 2008, during a short, intensive storm event. Two bottom sediment samples were collected on August 18, 2008: In the thick sediment layer in the pond center 10 m from the inlet, and in the much thinner sediment layer by the shore 10 m from the pond outlet [Fig. 3(b)]. Samples were passed sequentially through 2-mm and 150-μm filters to eliminate coarse sand (Vollertsen 2010). The inorganic particle size distribution (PSD) was analyzed with a Malvern Mastersizer 2000, owned by the Icelandic Meteorological Office. 90% of inflowing sediments were clay or silt particles

Table 2. PSD and Selected Shear Stress for Particle Resuspension

	Sampling location			
PSD (μm)	Inflow water	Near inlet sediments	Near outlet sediments	$\tau_{cr,Qin}$ (Pa)
d_{10}	2.2 ± 0.4	2.5	1	0.04
d_{25}	6.0 ± 1.6	8	3	0.06
d_{50}	13 ± 4	23	8	0.08
d_{75}	29 ± 9	57	18	0.11
d_{90}	52 ± 18	140	40	0.14

Note: Critical shear stress for resuspension of particles in inflow.

($d_{90} < 60$ μm, Table 2), in accordance to previously documented particulate sizes in road runoff with TSS less than 100 mg/L (Andral et al. 1999; Furumai et al. 2002). The bed sediments near the pond inlet skewed toward larger grain sizes in accordance with selective particle deposition. The bed sediments near the pond outlet were considerably finer, indicating that the larger particle fractions had already settled. The required bed-shear stress for resuspending inflowing particles of different sizes was on the order of 0.04–0.15 Pa [Eqs. (15) and (16), $\phi = 35°$, $s = 2.6$, $\nu = 1.5 \times 10^{-6}$ m^2/s]. The lower and upper limits correspond to critical shear stress needed to erode the top 0.3 to 3-mm sediment layer of a stormwater pond (Bentzen 2010).

Event Mean Results

Removal of TSS during four runoff events (Fig. 4), representing varying wind and hydraulic loadings, is summarized in Table 3. The start of a throughflow event was taken when hourly inflow exceeded 2.5 L/s, and the end when Q dropped below 2 and 1 L/s for the winter and spring storms, respectively. The outflows represent 15–94% of the inflowing volume, the lower bound reflecting the difficulties of sampling water during the long tails of the outflows. Event mean metrics were calculated as weighted averages with throughflows.

Table 3 shows that wind-induced short-circuiting was predicted to occur within 2–6 h, corresponding to $SCI < 0.04$, which is an

Table 3. Event Mean Summary

	Hydrology				Wind metrics				Particulate removal		
Event	*Start*	*T* (h)	V_{in} (m³)	V_{out}/V_{in} (%)	t_{sc} (h)	*SCI*	Pe_z	Pe_x	χ_{10}	$N_{f,50}$	R.E.$_{EV}$	R.E.$_{meas}$
December 22	8:30	31.5	1,709	94	2.3	0.04	0.05	0.4	0.4	11	87	64
February 13	6:10	16.5	460	42	5.6	0.03	0.12	0.2	0.2	31	95	88
May 10	3:00	51.7	594	63	3.3	0.01	0.08	0.1	0.3	66	98	−2
May 28	4:00	20.7	244	15	3.2	0.01	0.07	0.1	0.1	72	98	52

order of magnitude lower than documented in stormwater ponds driven solely by throughflows (Persson 2000). The median size particles were vertically mixed during all events as $Pe_z \leq 0.2$. While entering pollution may be initially transported like plug flow with circulatory currents, it is well mixed within the time it resides within the pond reflected in $Pe_x < 2$. Resuspension of small clay size particles ($d_{10} = 2.2~\mu$m) was not likely in the center of the pond as $\chi_{10} < 1$. These wind metrics support the use of the EV model with no background concentration ($C_* = 0$) as a starting point.

The three columns to the right consider the pond's treatment performance. The event mean particle fall number ranged from 11 to 70, for which the analytical EV model [Eq. (23)] with 60% effective volume based on Bentzen et al. (2008) predicts over 87% hydraulic removal efficiency. The measured event mean removal efficiency, based on the ratio of event mean TSS concentrations in the in- and outflow ranged, however, from 88% during the February event to negative values during the low-intensity, long-duration May 10 storm, suggesting that the pond was a source of solids during that event. Background concentrations are, therefore, important in this pond.

Numerical Model Results

Quantification of Removal Reduction Mechanisms

The numerical counterpart of the EV model [Eq. (31)] was used to quantify removal inefficiencies associated with different wind mechanisms and to assess the parameters e and C_*. Model input data were 10-min measurements of water depth, in- and outflows. The surface area of the trapezoidal pond was adjusted for varying water depth. The quality of the simulations was assessed on the one hand with model errors, calculated as the event mean standard deviation between modeled and measured TSS in the pond effluent [Fig. 5(a)], and on the other hand with the event mean removal efficiency [Fig. 5(b)]. Four scenarios were considered: In Scenario

1 ($e = 1$, $C_* = 0$), the outflow concentrations were 7–8 mg/L lower than measured and simulated removal efficiency 87–98%. Accounting for ineffective volume ($e = 0.6$, Scenario 2), the standard errors reduced moderately by 1 mg/L, and removal efficiencies by 3–7%, for the two high intensity winter storms ($N_{f,50} \leq 30$, Table 2). Testing the model sensitivity to varying e, the lowest modeling errors were found for $e = 0.6$ and 0.7 for the December and February storms, respectively. This range compares well with the 3D numerical tracer results of Bentzen et al. (2008) in a similar sized, shallower pond. Effective volume, however, minimally affected the two May simulations as expected with $N_{f,50} \approx 70$. Incorporating a constant background concentration ($C_* > 0$, Scenario 3), implying that time-varying external factors such as wind and chemical loading do not influence background concentration within an event, model errors were reduced to 2–4 mg/L in all four events. The simulated removal efficiencies were within 1–6% of those measured. Assuming an independent pre-event background concentration ($C_0 \neq C_*$, Scenario 4) gave similar event mean results as Scenario 3, but captured best the time variability of outflowing TSS, discussed in the next section. To summarize, wind-related hydraulic inefficiencies (BSM and EV) accounted for an 8–20% reduction in removal performance during moderate particle fall numbers ($N_{f,50} = 10$–30), and 5% during high particle fall numbers ($N_{f,50} \approx 70$). Background concentrations were important at this site, contributing to an additional 4–100% removal reduction.

Model Applicability

Fig. 6 compares the modeled TSS in the outflow for Scenario 4 to measurements during three individual events. In the December event [Fig. 6(a)], outflowing TSS peaked at the same time as inflowing TSS at $t \approx 17$ h. Stirred reactor simulations consistently predicted the timing of the peak concentration in outflow 3.5 h later than observed. The February event [Fig. 6(b)] was noteworthy in that the TSS effluent concentrations were high at the beginning of the storm (12 mg/L), then dropped abruptly down to 4 mg/L
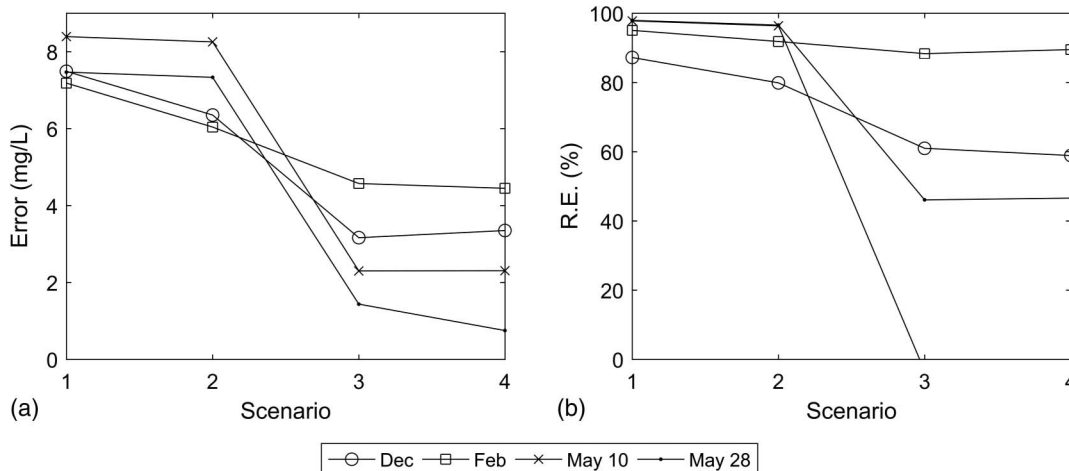

Fig. 5. (a) Simulated model error; (b) removal efficiencies for four scenarios; (1: *BSM*; 2: $e = 0.6$; 3: $C_* = C_0$; 4: $C_* \neq C_0$)
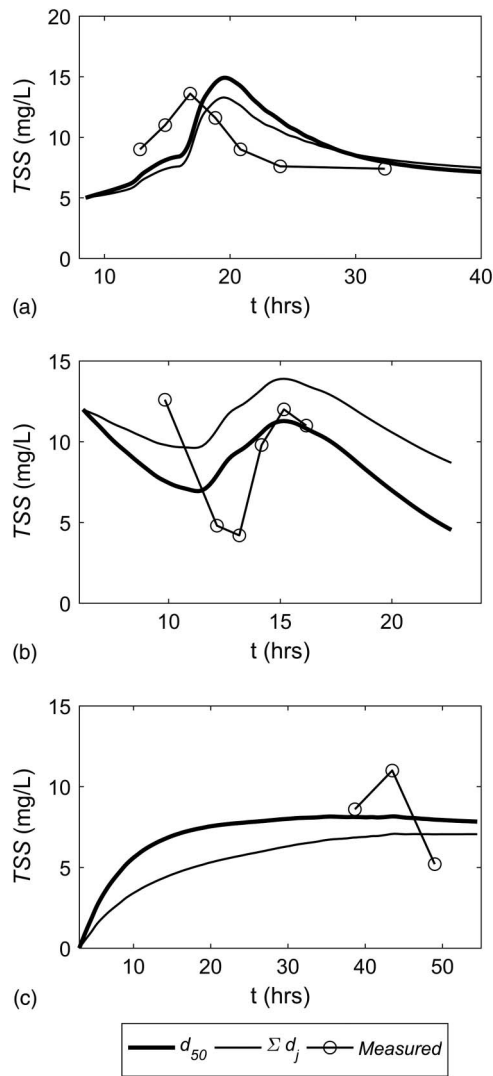
Fig. 6. Scenario 4 model simulations of outflowing TSS during (a) December (b) February c) May 10 events

TSS at $t = 13$ h concurrent with an increase in inflowing Na [Fig. 4(e)], before rebounding back to the original values. This drop was not linked to the wind, which remained steady until at $t \approx 16$ h [Fig. 4(c)]. The model simulated a milder decline in TSS than observed. Despite temporal deviations between measurements and simulations, event mean removal efficiency was modeled with 5% accuracy. The measured TSS effluent concentrations varied little during the two May storms, supported by simulations [Fig. 6(c)]. At $N_{f,50} \approx 70$, full removal potential was achieved and outflowing TSS were representative of background concentrations independent of the assumed initial condition [$C_0 = 0$, Fig. 6(c)].

To address the applicability of using solely the median diameter, d_{50}, simulations were also performed for the sum of three different size classes, d_{25}, d_{50}, and d_{75} (Table 2), with $PSD_j = 30, 40, 30\%$, respectively. The same PSD was used in the four events, as particle sizes in winter snowmelt or rain-on-snow events were not found to be statistically different between those in spring rainfall events (Westerlund and Viklander 2007). The particulate size distribution of the initial and background concentrations, $PSD_{0,j} = PSD_{*,j} = 60, 40$, and 0%, was chosen to reflect the fact that fine silt, and to a lesser extent, medium silt particles were likely to stay long enough in suspension to contribute to background concentrations (Fig. 2). Fig. 6 shows that the predicted effluent TSS concentrations varied similarly with time as those assuming d_{50}, but with a shift of 1–3 mg/L. This shift only affected the event mean removal efficiency for the two spring storms, producing a worse outcome than d_{50}. When assuming fewer degrees of variation ($C_* = C_0$, Scenario 3, not shown), the removal efficiencies predicted for mean versus the sum of the diameters matched within 2%. This suggests that using a median diameter is a good starting choice for an analytical bulk model. Modeling different size classes warrants more input data, e.g., the particle size density function of the initial ($PSD_{0,j}$) and background ($PSD_{*,j}$) concentrations inside the pond.

Background Concentrations

Table 4 presents the calibrated background and initial concentrations in relation to selected hydrologic, wind, and chemical conditions leading to and during the events. Calibrated model background concentrations were <8 mg/L during events, which corresponds to the lower limit of the reported 10–20 mg/L range in stormwater retention ponds receiving low sediment fluxes (<200 mg/L TSS, Barrett 2008). The model background concentrations compared generally well with the minimum TSS measured in the pond effluent. No correlation was found between event mean background concentration and wind speed, which varied from 7–11 m/s between events. However, a negative correlation was found between background TSS and Na concentrations in the pond effluent during events in Scenarios 3 and 4 ($R^2 > 0.7$). The use of road salt as a deicing agent in cold climates may contribute to low background concentration. Salt is known to promote flocculation of fine clay particles (Sutherland et al. 2015).

Initial TSS concentration, C_0, was strongly positively correlated ($R^2 \approx 1$) with wind speed prior to the event, which varied considerably in strength (but not in direction). While wind currents were not likely to generate basin-scale resuspension from the bed (Table 3), localized wind-induced resuspension may be present in the shallows that contribute to background concentration. A weaker, negative correlation ($R^2 \approx 0.4$) was found between C_0 and the antecedent dry weather period (ADWP), supporting the notion of wash loads from one event contributing to background concentrations in the next. Initial background concentration was not correlated to wind duration before event ($T > 5$ h). This preliminary analysis, conducted over a limited number of events,

Table 4. Modeled Background and Initial Concentrations in the Context of Meteorological and Chemical Conditions during and before Events

| Event | During event | | | | | Before event | | | | | |
	W_2 (m/s)	Na_{out} (mg/L)	min(TSS$_{out}$) (mg/L)	$C_{*Sc.3}$ (mg/L)	$C_{*Sc.4}$ (mg/L)	ADWP (days)	W_2 (m/s)	θ_w (°)	T (h)	Wind trends	$C_{0\,Sc.4}$ (mg/L)
December 22	11	106	7.4	6	7	7	3.3	88	15.5	Steady	5
February 13	8.1	184	4.2	3	0	5	10.3	75	20	Steady	12
May 10	6.6	37	5.2	8	8	5	2.3	120	5	Steady	N/A
May 28	8.9	35	6.4	7	6	2	7.8	106	6	Increasing	10
R^2_{C*3}	0.03	0.9	0.2	—	R^2_{C0}	0.4	1.0	0.03	0.01	—	—
R^2_{C*4}	0.01	0.7	0.4	—	—	—	—	—	—	—	—

identifies wind speed and salt as potential external factors for background concentrations in cold climate stormwater ponds. Detailed sampling and analysis over more events encompassing a greater range in wind conditions is required to verify this hypothesis.

Summary and Conclusions

Traditionally, hydraulic inefficiencies contributing to a reduced treatment performance in stormwater ponds have been related to structural design parameters, such as low length-to-width ratios, irregular shape and small separation between inlets and outlets. Building upon recent research identifying wind as the dominant flow driver in a shallow stormwater pond, this study quantified the impact of different wind mechanisms on particle removal efficiency with an analytical bulk model. Model solutions, corroborated by event-based field measurements, suggest that wind stirring, basin-scale mixing, and short-circuiting, can lead to an 8–20% reduction in solids treatment performance in an optimally designed pond for $N_f = 10$–30. Wind most severely constrains the removal of the smallest clay and silt particles, with diameters under 6 μm, which play an important role in aquatic ecology, both because of their higher toxicity and higher pollutant concentrations. These particles are easily vertically mixed, require weeks to settle, and can contribute to background concentrations (or wash loads) because of the wind. In the worst case scenario, the pond can become a source of materials if the wind is strong enough to resuspend materials from the bed.

The model was validated against TSS data in an oval pond, with a length-to-width ratio of 4:1 and a long separation between inlet and outlet. The pond was heavily influenced by wind, with short-circuiting currents and basin-scale mixing occurring quickly compared to throughflows ($SCI < 0.04$, $Pe_x < 0.4$). Visual observations of preferential sediment accumulation near the pond inlet, as well as empirical estimates of wind-induced shear bed stress, suggested that the combination of a water depth >1.7 m and small wind fetch (112 m) limited basin-scale remobilization of bed sediments. Despite this, calibrated model background concentrations prior to four runoff events were positively correlated with wind speed, which could be explained by localized resuspension in downwind shallows. Background TSS concentrations during the events were, however, correlated with Na concentrations, indicative of the use of road salt in a cold climate. Hence the study confirms wind as a driver for background concentration, but that chemical factors may be important as well.

A stirred reactor model with 60% effective volume was found to predict with 6% accuracy the measured bulk treatment of TSS. This type of idealized model may, therefore, serve as a first order tool to predict event mean removal of median size particles in small wind-dominated ponds. This claim inherently means that wind circulation and mixing limit treatment in ideal ponds by reducing their effective volume. Conversely, wind may improve the treatment in ponds with a low length-to-width ratio or little separation between inlets and outlets by increasing their effective volume to 60–70%. The stirred reactor model did not capture the exact timing of peak TSS concentrations, however, and tended to smooth out increases and drops in outflowing TSS. This suggests that background concentration and/or hydraulic regime may have varied within an event. To fully understand time varying particulate dynamics in wind driven ponds may, therefore, require a coupled 3D hydrodynamic-sediment transport model, validated with high resolution, temporal field data that include particle size distributions within and between events.

References

Andradóttir, H. Ó., and Mortamet, M. L. (2016). "Impact of wind on stormwater pond hydraulics." *J. Hydraul. Eng*, 10.1061/(ASCE)HY.1943-7900.0001150, 04016034.

Andradóttir, H. Ó., and Vollertsen, G. E. (2015). "Heavy metals in suburban road runoff in a rainy cold climate." *J. Environ. Eng.*, 10.1061/(ASCE)EE.1943-7870.0000894, 04014068.

Andral, M. C., Roger, S., Montrejaud-Vignoles, M., and Herremans, L. (1999). "Particle size distribution and hydrodynamic characteristics of solid matter carried by runoff from motorways." *Wat. Environ. Res.*, 71(4), 398–407.

Barrett, M. E. (2008). "Comparison of BMP performance using the international BMP database." *J. Irrig. Drain Eng.*, 10.1061/(ASCE)0733-9437(2008)134:5(556), 556–561.

Bengtsson, L., and Hellström, T. (1992). "Wind induced resuspension in a small lake," *Hydrobiologia*, 192(2–3), 167–181.

Bentzen, T. R. (2010). "3D modelling of transport, deposition and re-suspension of highway deposited sediments in wet detention ponds." *Water Sci. Technol.*, 62(3), 736–742.

Bentzen, T. R., Larsen, T., and Rasmussen, M. R. (2008). "Wind effects on retention time in highway ponds." *Water Sci. Technol.*, 57(11), 1713–1720.

Bentzen, T. R., Larsen, T., and Rasmussen, M. R. (2009). "Predictions of re-suspension of highway detention pond deposits in interrain event periods due to wind-induced currents and waves." *J. Environ. Eng.*, 10.1061/(ASCE)EE.1943-7870.0000108, 1286–1293.

Dhamotharan, S., Gulliver, J. S., and Stefan, H. G. (1981). "Unsteady one-dimensional settling of suspended sediment." *Wat. Res. Res.*, 17(4), 1125–1132.

Fischenich, C. (2001). "Stability thresholds for stream restoration materials." *EMRRP Technical Notes Collection, ERDC TN-EMRRP-SR-29*, U.S. Army Engineer Research Center, Vicksburg, MS.

Furumai, H., Balmer, H., and Boller, M. (2002). "Dynamic behavior of suspended pollutants and particle size distribution in highway runoff." *Water Sci. Technol.*, 46(11–12), 413–418.

Gunnarsson, J. O., and Sigurdsson, G. (2007). "Styrkur mengunarefna í ofanvatni og virkni settjarnar við Víkurveg vatnsárið 2005/2006 (Eng. Runoff pollutant strength and wet retention pond efficiency at Víkurveg for the water year 2005/2006)." *Reykjavík: Orkustofnun (JOG-GS-2007/001)* Orkustofnun, Reykjavík, Iceland (in Icelandic).

Hazen, A. (1904). "On sedimentation." *ASCE Trans.*, 53(2), 45–71.

Hossain, M. A., Alam, M., Younge, D. R., and Dutta, P. (2005). "Efficiency and flow regime of a highway stormwater detention pond in Washington, USA." *Water Air Soil Pollut.*, 164(1–4), 79–89.

Icelandic Meteorological Office. (2009). "Volumetric flow measurements at Víkurvegur pond in 2008-2009." Icleandic Meteorological Office, Reykjavík, Iceland.

Kachhwal, L. K., Yanful, E. K., and Rennie, C. D. (2012). "A semi-empirical approach for estimation of bed shear stress in a tailings pond." *Environ. Earth Sci.*, 66(3), 823–834.

Kadlec, R. H. (2000). "The inadequacy of first-order treatment wetland models," *Ecolog. Eng.*, 15(1–2), 105–119.

Li, Y., Deletic, A., and Fletcher, T. D. (2007). "Modelling wet weather sediment removal by stormwater constructed wetlands: Insights from a laboratory study." *J. Hydrol.*, 338(3–4), 285–296.

Persson, J. (2000). "The hydraulic performance of ponds of various layouts." *Urban Water*, 2(3), 243–250.

Pitt, R., Field, R., Lalor, M., and Brown, M. (1995). "Urban stormwater toxic pollutants: Assessment, sources and treatability." *Water Environ. Res.*, 67(3), 260–275.

Sansalone, J. J., and Buchberger, S. G. (1997). "Characterization of solid metal element distributions in urban highway stormwater." *Water Sci. Technol.*, 36(8–9), 155–160.

Sutherland, B. R., Barrett, K. J., and Gingras, M. K. (2015). "Clay settling in fresh and salt water." *Environ Fluid Mech.*, 15(1), 147–160.

Thackston, E. L., Shields, F. D., Jr., and Schroeder, P. R. (1987). "Residence time distributions of shallow basins." *J. Environ. Eng.*, 10.1061/(ASCE)0733-9372(1987)113:6(1319), 1319–1332.

Tsai, D. D.-W., and Chen, P. H. (2013). "Differentiation criteria study for continuous stirred tank reactor and plug flow reactor." *Theor. Found. Chem. Eng.*, 47(6), 750–757.

Vista Engineering. (2009). "Meteorological data at weather station Ulfarsa 2008–2009, collected on behalf of the City of Reykjavík." ⟨http://vista.is⟩ (Jan. 1, 2010).

Vollertsen, G. E. (2010). "Removal of heavy metals in a wet detention pond." Master's thesis, Faculty of Civil and Environmental Engineering, Univ. of Iceland, Reykjavík, Iceland, 105.

Westerlund, C., and Viklander, M. (2007). "Particles and associated metals in road runoff during snowmelt and rainfall." *Sci. Tot. Environ.*, 362(1–3), 143–156.

Wong, T. H. F., Fletcher, T. D., Duncan, H. P., and Jenkins, G. (2006). "Modelling urban stormwater treatment—A unified approach." *Ecol. Eng.*, 27(1), 58–70.